

IGNITION, TRANSITION, FLAME SPREAD IN MULTIDIMENSIONAL CONFIGURATIONS IN MICROGRAVITY

TAKASHI KASHIWAGI, William E. Mell, Kevin B. McGrattan, Howard R. Baum
National Institute of Standards and Technology, Gaithersburg, Maryland

Sandra L. Olson
NASA Lewis Research Center, Cleveland, Ohio

and

Osamu Fujita, Masao Kikuchi, Kenichi Ito
Hokkaido University, Sapporo, Japan

Introduction

Ignition of solid fuels by external thermal radiation and subsequent transition to flame spread are processes that not only are of considerable scientific interest but which also have fire safety applications. A material which undergoes a momentary ignition might be tolerable but a material which permits a transition to subsequent flame spread would significantly increase the fire hazard in a spacecraft. Therefore, the limiting condition under which flame cannot spread should be calculated from a model of the transition from ignition instead of by the traditional approach based on limits to a steady flame spread model. However, although the fundamental processes involved in ignition have been suggested^[1,2] there have been no definitive experimental or modeling studies due to the flow motion generated by buoyancy near the heated sample surface.

Almost all previous works have studied ignition and flame spreading separately^[3,4,5]. In previous flame spread studies, time-dependent flame spread models are limited to upward flame spread over a vertically oriented material surface in normal gravity which is generally assumed to be two-dimensional. Almost all detailed flame spread models^[6,7,8] were based on a steady-state flame spread rate and, as far as we are aware, there are no previous studies of three-dimensional time-dependent flame spread which is initiated from a small, localized ignited area. This scenario is most common in real fires. Thus, the study of localized ignition and the subsequent transition to flame spread in multidimensional configurations in a microgravity environment is needed to obtain new information for understanding transition and flame growth mechanisms.

Smoldering (non-flaming glowing combustion) is one of the common modes of initiation of fires; it might provide potentially hazardous conditions due to its high CO yield, but there are only a limited number of studies available in microgravity, in particular for surface smoldering phenomena. Although the heat release rate from smoldering is smaller than that from flaming, the temperature of the smoldering front is as high as 800 °C or more and the induced buoyant flow velocity from the high temperature smoldering front is roughly 20 cm/s in normal gravity. Since the supply of oxygen to the smoldering front is one of the critical parameters which control smoldering spread rate, it is expected that surface smoldering growth behavior at slow external flow of up to 5 cm/s in microgravity could be significantly different from that in normal gravity.

In this study, microgravity experiments which required longer test times such as in air and surface smoldering experiments were conducted in the space shuttle STS-75 flight; shorter experimental tests such as in 35% and 50% oxygen were conducted in the droptower in the Japan Microgravity Center, JAMIC. Their experimental data along with theoretically calculated results from solving numerically the time-dependent Navier-Stokes equations are summarized in this paper.

Experimental Description and Results

The experimental module, shown schematically in Figure 1, uses a small fan to generate a low flow velocity of up to 6.5 cm/s through the test section. The test section is 85 mm wide x 95 mm high x 171 mm long. A near-infrared tungsten/halogen radiant heater is used to ignite a circular area in the center part of a sample in the three-dimensional configuration. The power to the lamp was measured during each test and it was turned off after ignition at a preset time. The emission spectrum of the lamp was measured from

NASA Conference Publication 10194;
Microgravity Combustion Workshop, Fourth (4th)
International. Proceedings. National Aeronautics and
Space Administration, Lewis Research Center. NASA
Conference Publication 10194. May 19-21, 1997,
Cleveland, OH, 411-416 pp, 1997.

2 to 20 μm using a FTIR. A 10 cm x 8.7 cm sheet of Whatman 44¹ ashless filter paper was used as the sample. The center part of the sheet over the irradiated area was blackened to increase absorption of the incident beam from the lamp. The samples were ignited at a central location either by the focused beam from the lamp (three-dimensional configuration) or along a line by a heated wire to observe planar flame growth (two-dimensional configuration). A few samples were doped with a smolder promoting agent, potassium acetate, to study smolder propagation from a central ignition point. Six 0.05 mm diameter type K thermocouples and an ignitor wire (30 gauge Kanthal wire) were pre-installed across the sample on each sample holder. Four thermocouples were installed in the sample at the center, 2 cm and 4 cm downstream from the center and at 2 cm upstream. Two thermocouples were installed at 2 mm above the sample surface at 2 cm upstream and also at 2 cm downstream locations from the center. Color video pictures were taken in the direction normal to the sample surface to view changes in the flame shape and char pattern. Red diodes were used to illuminate the sample surface. Still color photographs were taken at an oblique angle to the sample by a motor-driven 35 mm camera.

Ignition was achieved in all tests using either a heated wire or a lamp. Radiative ignition by the lamp was quite reproducible and the results show that the ignition delay time was not significantly affected (within 10%) by the external flow velocities used in this study. The ignition delay time was $4.4 \pm 0.4\text{s}$ in air, $4.2 \pm 0.3\text{s}$ in 35% oxygen, and $3.8 \pm 0.2\text{s}$ in 50% oxygen. These ignition delay times included about 2.2s from power on to a point where the output of the lamp reached the designated flux. Ignition by a heated wire was less reproducible than that by the lamp due to changes in wire contact with the sample caused by the expansion of the wire as it heated. Ignition tended to occur at one face of the sample surface at first followed by the second ignition on the other face of the sample. The second ignition occurred very quickly in 50% oxygen but it took several seconds in air.

The transition from ignition to flame spread occurred in quiescent 35% and 50% oxygen but it did not occur in quiescent air. In the two-dimensional configuration, the transition from ignition to downstream flame spread never occurred; only the transition to upstream spread took place. This is clearly seen for the case in air at the external flow velocity of 5 cm/s as shown in Fig.2. In air, the color of the flame was blue and it became somewhat orange in 35% and 50% oxygen. The brightness and the length of the flame increased with an increase in oxygen concentration and also in external flow velocity. The tail of the flame extended further downstream and char was even formed downstream near the initially ignited region. However, downstream sample temperatures measured by thermocouples did not exceed over about 330 °C compared to about 500 °C for upstream sample temperatures beneath the traveling upstream flame front. In the three-dimensional configuration, the flame spread pattern was strongly affected by oxygen concentration and flow velocity. In air, at 0.5 cm/s, a small flame spread only upstream maintaining the initial flame shape from shortly after ignition. The flame never grew laterally from its initial width and this is also clearly seen in the growth pattern of char in Fig. 3a. However, the flame and char growth patterns did grow laterally outward with an increase in the external velocity, as shown in Figs 3b and 3c. At 2 cm/s, the flame had a crescent shape and the char growth pattern was initially an elongated circle pointing upstream; at later times, it became fan-shaped. At 6.5 cm/s, the shape of the flame became like a horseshoe with the tails of the horseshoe flame extending downstream. The char pattern became a circle elongated in the upstream direction with a relatively flat downstream side. A similar shape was also observed in 35% and 50% oxygen concentrations at 5 cm/s external flow velocity. A major difference in flame shape between air in this study and 50% oxygen concentration is that a spreading spherical flame was observed in a quiescent condition in 50% oxygen concentration compared with no transition to flame spread in the air case. Therefore, at low external velocities, the char patterns were more or less spherical in 50% oxygen concentration instead of the narrow strip char pattern observed in the air case. The observed trend of opening the angle of the char pattern in the upstream direction with an increase in external flow velocity of air in microgravity is quite different from the narrowing angle trend of the downstream flame with an increase in external flow velocity in normal gravity. However, it is expected that further increase in external velocity in microgravity would eventually reduce the upstream flame spread rate and be sufficient to promote downstream flame spread. Thus, this observed trend of the char pattern is unique and should occur only at low external flow velocities and low oxygen concentrations, such as in air, in microgravity.

The histories of the location of the char front spreading upstream along the centerline could be fit reasonably well by linear equations with time. Thus, apparently steady-state-like upstream char front spread rates along the centerline were obtained for each experiment. The results are shown in Fig.4. Some caution is needed in comparing the results between the two-dimensional configuration and the three-dimensional configuration due to the transient nature of the three-dimensional flame and there are not sufficient data for the case in air in the two-dimensional configuration. The results show that the upstream char spread rate appears

¹Certain company products are mentioned in the text in order to specify adequately the experimental procedure and equipment used. In no cases does such identification imply recommendation or endorsement by the National Institute of Standards and Technology and NASA, nor does it imply that the products are necessarily the best available for the purpose.

to reach a plateau in the flow velocity range of about 5 - 10 cm/s, where the spread rate becomes independent of the external flow velocity^[9]. Although the difference between the two-dimensional configuration and the three-dimensional configuration in 50% oxygen is within the scatter of the data, the results in 35% oxygen indicate that the spread rate in the three-dimensional configuration is faster than in the two-dimensional configuration due possibly to a larger oxygen supply at the curved flame front. In the regime where oxygen supply is the critical rate-controlling process, a curved flame front has a larger area for incoming oxygen to reach. This could be more clearly seen in air but unfortunately there were not enough data in the two-dimensional configuration. Some care is needed to make sure to generate a planar flame in the two-dimensional configuration. If a planar flame is not generated, the result is instead a three-dimensional configuration.

Four smoldering experiments were conducted in the space shuttle STS-75 with ignition initiated at the center of the sample by the lamp. The sample was doped with potassium ions to enhance char formation and char oxidation (4.2 weight % \pm 5% in spatial non-uniformity). Although a ring-shaped smoldering front was initially observed in normal gravity (the ring-shaped front gradually deformed due to induced buoyant flow from the hot smoldering surface), unexpected, very complex finger-shaped char patterns with localized smoldering fronts at the finger tips were observed in microgravity; such patterns are seen in Fig.5. In these pictures, the white spots are the localized smoldering fronts. The direction of growth of the char pattern was mainly upstream; higher external flow velocity tends to increase the number of localized smoldering fronts, the number of fingers, and also the frequency of bifurcations from each finger. At present it is not clear what caused this complex pattern.

The flame spread behavior along the open edges of the paper sample was studied at external flow velocities of 2, 3, and 5 cm/s in air using a narrow sample, 4 cm in width, in the same sample holder. Ignition was achieved by the lamp illuminating the center of the sample; initially, the flame spread radially upstream. Once the flame reached the open edges of the sample, the flame at each edge spread much more rapidly than the flame along the center line. At the open edges of the sample, oxygen supply to the flame (almost 360°) and energy feedback from the flame to the sample (from three sides) are much larger than that for the flame along the center of the sample (about 180° for oxygen supply and only two sides for energy feedback).

Theoretical Calculation

A complete description of the mathematical model has been given in Ref. [10]. The gas phase is governed by the conservation equations of mass, momentum, energy and species (fuel gases and oxygen) under low Mach number combustion and heat transfer conditions. In past work (two-dimensional configuration), it was assumed that the velocity field was approximated by a potential flow^[10,11]. Now, the full Navier-Stokes form of the momentum conservation equation (in three-dimensional configuration) is solved. However, the potential flow approximation is used to apply boundary conditions since the rapid expansion at ignition cannot be treated properly with conventional zero gradient boundary conditions. The uniform inlet flow condition is specified at the upstream edge of a paper sample and a boundary layer along the sample surface is calculated. The gas phase oxidation reaction is represented by a global one step reaction characterized by a second order Arrhenius rate equation. The pre-exponential factor is $5.0 \times 10^9 \text{ cm}^3/(\text{g}\cdot\text{s})$ and the activation energy is 67 kJ/mol. The heat of combustion is 35 kJ/g, and the stoichiometric constant is 3.57. These values are the same as those used in the two-dimensional study^[10]. It has been observed that the ignition and transition to flame spread are very sensitive to the choice of the gas phase reaction constants. The present choice is guided by a desire to roughly match flame spread rates with the experiments of Olson^[5]. However, the objective of the study is not necessarily to duplicate experimental results exactly by manipulating the model parameters, but rather to deduce trends of the transient phenomena.

The sample used in the experiments is more thermally stable than the paper used in our previous study^[10,11]. Its thickness is 0.13 mm, area density 5.7 mg/cm² and specific heat 0.96 J/(g·K). It is assumed that this value of specific heat applies to the char and ash, as well, and that it increases linearly with temperature. It is assumed that the sheet is thermally-thin and also of uniform composition through its depth. Radiative loss from the sample surface is included but radiation from the flame is not included in the model, and the emissivity of the sample is estimated to be 0.6. The pyrolysis of the cellulosic sheet is described by a slightly exothermic global pyrolysis reaction, an exothermic global thermal oxidative degradation reaction, and an exothermic global char oxidation reaction. The kinetic constants for each degradation reaction were derived with the same type of thermogravimetric analysis used in our previous study^[12].

The equations for the continuity, momentum, gas phase temperature and two species concentrations are written in finite difference form and solved with a simple time splitting scheme in which it is assumed that the oxidative reaction occurs over a small part of the overall time step, and the convective and diffusive terms are differenced and updated with an ADI (Alternating Direction Implicit) scheme. The momentum equation is solved with a simple projection method which relies on the prescription of the velocity field at the boundary of the computational domain. This boundary velocity is provided by the potential flow approximation. A Poisson

equation for pressure is solved with a direct solver. For the simulations described below, the computational domain was 10 cm in the windward direction, 5 cm spanning half of the lateral direction and 5 cm in the normal direction. Symmetry is assumed about the plane which is spanned by vectors normal to the paper surface and parallel to the wind direction. Also, the paper itself is assumed to be a plane of symmetry. A typical grid contains about 260,000 cells (128x64x32), and the calculations require about 48 hours of CPU time on a current generation workstation for a 5 second simulation of the events.

A typical result of flame spread behavior in a 33% oxygen atmosphere in the two-dimensional configuration is shown in Fig.6. The sample is ignited at the center part of the sample by a prescribed external radiant flux distribution (similar to the experimentally used lamp in the three-dimensional configuration) across the sample. At a quiescent condition and 1 cm/s flow, no transition from ignition to flame is achieved in the calculation. From 2 cm/s to 12 cm/s flow, the transition is achieved and steady flame spread is calculated only toward upstream which is the same trend as that observed in the experiment as shown in Fig.2. The char pattern shown in Fig.2 is very similar to that shown in Fig.6. The calculated upstream char spread rate with respect to external flow velocity is shown in Fig.7. From about 5 cm/s to 12 cm/s flow, the char spread rate is nearly independent of external flow velocity and this trend is consistent with the data shown in Fig.4 and previous experimental results^[5]. In a atmosphere of quiescent 50% oxygen in the three-dimensional configuration, the results show a flame of initially hemispherical dome shape. The top part of the flame eventually opens as it propagates far from the ignited area in the outward direction^[13]. Although this behavior of the flame appears to be reasonable, the opening of the top part of the flame was not observed due to lack of available test time, 10s, in the droptower. At 5 cm/s flow, the initial shape of the flame is similar to the quiescent case since the flow field is dominated by the rapid thermal expansion of the flaming ignition. However, after ignition the external flow begins to reshape the flame into a horseshoe pointed into the imposed flow as shown in Fig.8. The calculated char pattern for this case is similar to that shown in Fig. 3c but the flame in 50% oxygen is much brighter than that in air. The history of the upstream char front in 33% and 50% oxygen concentration in the three-dimensional configuration shows nearly linear growth with time after the transition from ignition. The relationship between the calculated upstream char spread rate and external flow velocity is shown in Fig.7. The symbols with a x mark indicate that ignition and some transition occurred but the flame died before spreading beyond the irradiated area. A comparison of the upstream char spread rate between the two-dimensional configuration and the three-dimensional configuration indicates a trend in which, at low external flow velocities, only the three-dimensional configuration appears to favor the transition and subsequent flame spread. This trend is similar to the case for 35% oxygen shown in Fig.4. However, the difference in the char spread rate between the two-dimensional configuration and the three-dimensional configuration is very small with the values of the gas phase kinetic constants used in this study. This difference tends to become less at higher oxygen concentration such as in 50% oxygen as shown in Figs. 4 and 7. In order to confirm this trend further, calculation at lower oxygen concentration is planned. Also, a proposal was written to conduct more experiments in the two-dimensional configuration in air.

Acknowledgments

This study is supported by the NASA Microgravity Science Program under the Inter-Agency Agreement No. C-32001-R. The JAMIC experiments were funded by the New Energy and Industrial Technology Development Organization through the Japan Space Utilization Promotion Center.

References

1. Kashiwagi, T. *Fire Safety J.* 3: 185-200(1981).
2. Muto, N., Hirano, T. and Akita, K. *Seventeenth Symposium (International) on Combustion*, The Combustion Institute, Pittsburgh, 1183-1190(1978).
3. Bhattacharjee, S and Altenkirch, R.A. *Twenty-Third Symposium (International) on Combustion*, The Combustion Institute, Pittsburgh, 1627-1633(1990).
4. Frey, A.E. and Tien, J.S., *Combust. Flame*, 36: 263 -289(1979).
5. Olson, S.L. *Combust. Sci. Tech.* 76:233-249 (1991).
6. Di Blasi, C., Crescitelli, S. and Russo, G. *Fire Safety Science- Proceedings of the Second International Symposium*, p119-128(1989).
7. Bhattacharjee, S., Altenkirch, A., Srikantaiah, N., and Vedhanayagam, M. *Combust. Sci. Tech.* 69:1-15(1990).
8. Ferkul, P.V. and Tien, J.S. *Combust. Sci. Tech.* 99:345-370(1994).
9. de Ris, J.N. , *Twelfth Symposium (International) on Combustion*, The Combustion Institute, Pittsburgh, pp.241-252(1969)
10. Nakabe, K., McGrattan, K.B., Kashiwagi, T., Baum, H.R., Yamashita, H., and Kushida, G., *Combust. Flame*, 98:361-374(1994)
11. McGrattan, K.B., Kashiwagi, T., Baum, H.R., and Olson, S.L., *Combust. Flame*, 106:377-391(1996).
12. Kashiwagi, T. and Nambu, H., *Combust. Flame*, 88:345-368(1992).
13. Kashiwagi, T., McGrattan, K.B., Olson, S.L., Fujita, O., Kikuchi, M., and Ito, K., "Effects of Slow Wind on Localized Radiative Ignition and Transition to Flame Spread in Microgravity" to be published in *Twenty-sixth Symposium (International) on Combustion*, The Combustion Institute, Pittsburgh, (1997).

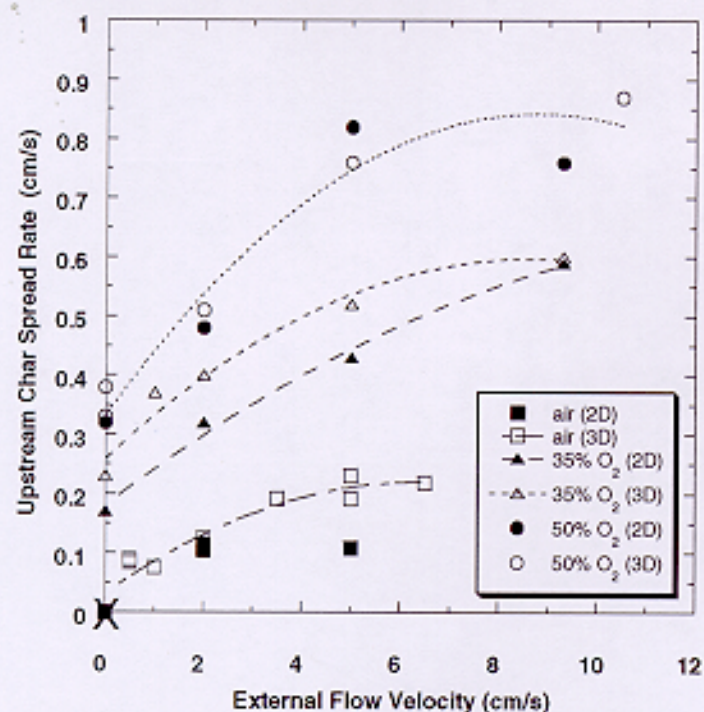


Fig. 4 Experimental upstream char spread rate vs flow velocity

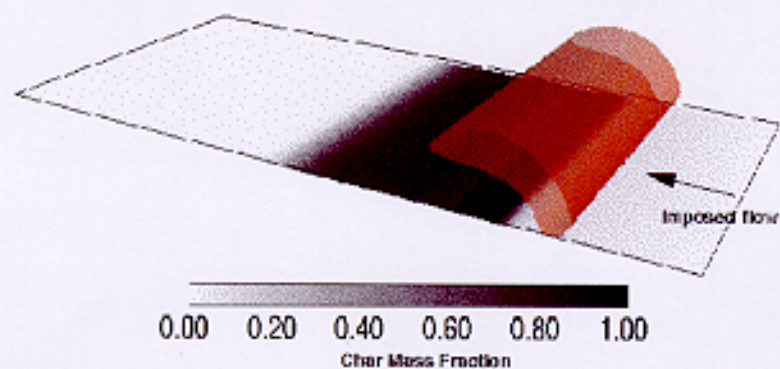


Fig. 6: 2D 5 cm/s (Calculation)



Fig. 5: Smoldering char pattern with smoldering fronts in air, 2 cm/s flow from right

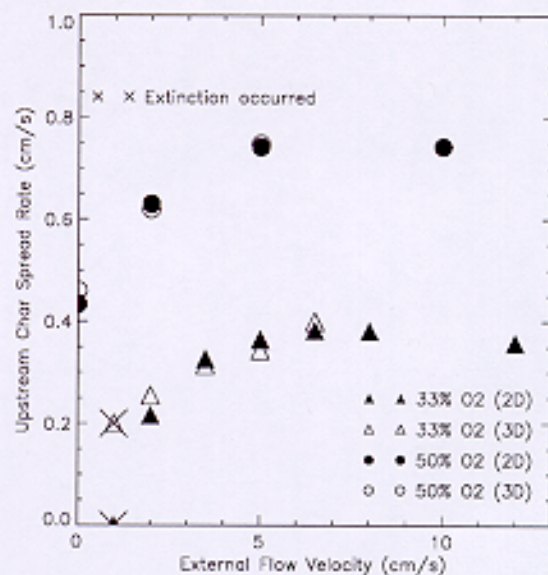


Fig. 7 Calculated upstream char spread rate vs external flow velocity

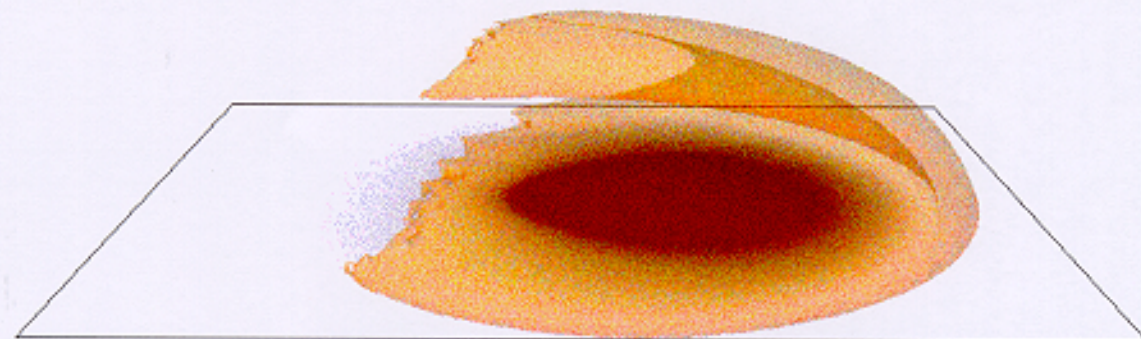


Fig. 8: Calculated flame and char pattern in 3D configuration, 5 cm/s in 50% oxygen

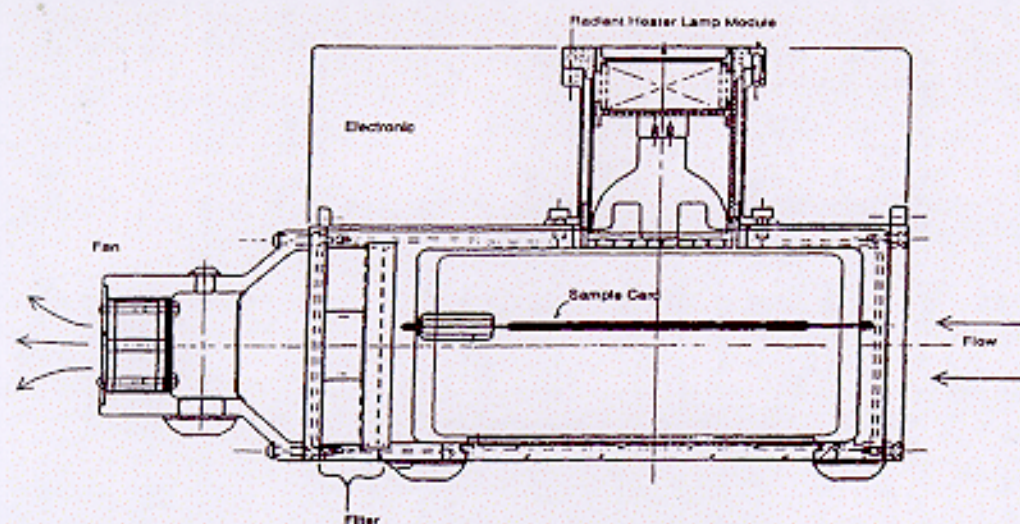


Figure 1 Schematic cross section view of hardware

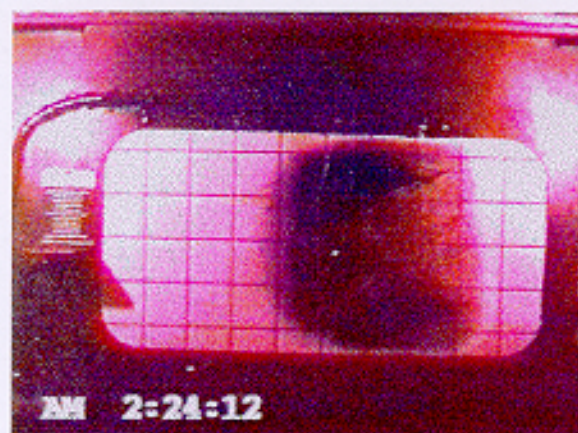


Fig. 2: Experimental 2D spread in air, 5 cm/s flow from right



Fig. 3a: Experimental 3D spread in air, 0.5 cm/s flow from right

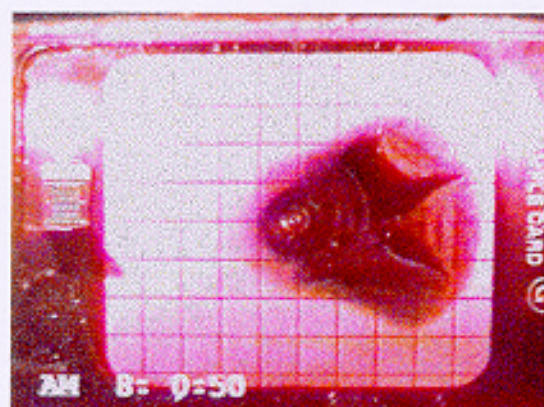


Fig. 3b: Experimental 3D spread in air, 2 cm/s flow from right

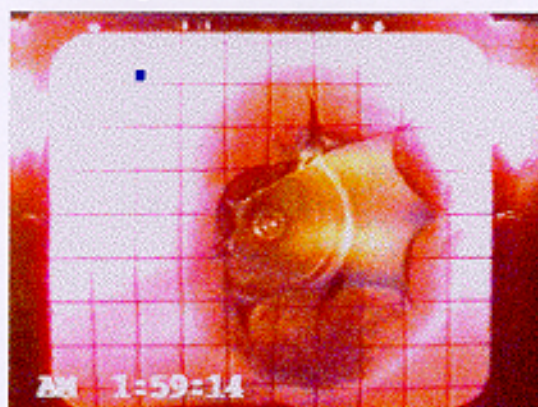


Fig. 3ci: Experimental 3D spread in air, 6.5 cm/s flow from right